An International Journal of Optimization and Control: Theories & Applications
ISSN: 2146-0957 eISSN: 2146-5703
Vol.16, No.4, pp.1404-1420 (2026)
https://doi.org/10.36922/IJOCTA026220100

RESEARCH ARTICLE

Flat lower envelopes solve bounded monomial convexification on two-variable cones

Yaoran Yang and Yutong Zhang*

School of Mathematics, Sichuan University, Chengdu, China
yangyaoran@stu.scu.edu.cn, yutongzhang@stu.scu.edu.cn

ARTICLE INFO

Article History:
Received: May 31, 2026
Revised: June 11, 2026
Accepted: June 15, 2026
Published Online: June 29 2026

Keywords:
Convex envelope
Monomial
Two-variable cone
Global optimization
Epigraph convexification
Reproducible numerical experiments

AMS Classification 2020:
90C26; 90C30; 52A20; 26B25

ABSTRACT

Bounded monomial sets are basic relaxable objects in deterministic global optimization. Belotti's 2025 *Mathematical Programming* article established the upper envelope for two-variable cones and the lower envelope in dimension two, while leaving the lower envelope open in dimensions greater than two. We close this gap by proving that, in every dimension of at least three, the lower convex envelope over the bounded monomial set intersected with a two-variable cone is flat: after convexifying the restricted epigraph, the only lower constraint on the graph variable is the imposed lower value bound. The formula is independent of the upper value bound and the total homogeneity degree. The proof is based on a level-set convexification identity: every point in the monomial superlevel set inside the cone is either on the target level or an explicit convex combination of two points on that level. A single coordinate outside the constrained pair supplies the required compensation, which also explains why the result fails sharply in dimension two. Combining this lower-envelope formula with Belotti's known upper envelope yields the complete convex hull of the bounded graph for all homogeneity regimes in dimensions of at least three. We also give constructive certificates, separation conditions, a notation summary in the back matter, and reproducible numerical diagnostics showing that the two-point certificates are recovered to roundoff-level reconstruction accuracy over representative regimes.

1. Introduction

Let

$$f(x) = \prod_{k=1}^{n} x_k^{a_k}, \qquad a \in \mathbb{R}^n_{++}, \tag{1}$$

and let $0 \le \ell < u < \infty$. The bounded monomial set is

$$X_{\ell,u} := \{x \in \mathbb{R}^n_+ : \ell \le f(x) \le u\}. \tag{2}$$

For fixed distinct indices $i, j \in \{1, \ldots, n\}$ and scalars $0 < p < q$, define the two-variable cone

$$W_{ij} := \{x \in \mathbb{R}^n_+ : px_i \le x_j \le qx_i\}. \tag{3}$$

Belotti[1] studies the convex hull of the graph of (1) on $X_{\ell,u} \cap W_{ij}$. The paper gives the upper envelope for $n \ge 2$ and the lower envelope for $n = 2$, and explicitly leaves the lower envelope for W_{ij} as an open problem for $n > 2$. This note solves that open problem and gives the resulting full convex hull description in dimensions of at least three.

Equivalently, the open question addressed here is: for $n > 2$, determine the exact lower convex envelope of the bounded monomial over $X_{\ell,u} \cap W_{ij}$ and decide whether the upper value bound u changes that lower epigraph after convexification. Our answer is that the convexified projection is precisely S_ℓ and the lower envelope is the constant value ℓ throughout this projection.

The basic objects are the restricted graph

$$\mathcal{G}_{\ell,u} := \{(x, z) \in \mathbb{R}^n_+ \times \mathbb{R} : x \in X_{\ell,u} \cap W_{ij},\ z = f(x)\}. \tag{4}$$

the lower epigraph hull

*Corresponding Author

$$\mathcal{E}^-_{\ell,u} := \operatorname{conv}\big(\{(x,z) : x \in X_{\ell,u} \cap W_{ij},\ z \geq f(x)\}\big). \tag{5}$$

and the upper hypograph hull

$$\mathcal{E}^+_{\ell,u} := \operatorname{conv}\big(\{(x,z) : x \in X_{\ell,u} \cap W_{ij},\ z \leq f(x)\}\big). \tag{6}$$

The lower envelope is encoded by (5); the upper envelope is encoded by (6). The difficulty in[1] is that, after intersecting $X_{\ell,u}$ with (3), the set is bounded in dimension two but unbounded in every dimension $n > 2$. The main point of the present paper is that this unboundedness is not an obstacle to the lower envelope; it is the mechanism that makes the lower envelope collapse to a constant.

Our principal theorem is the following closed-form solution of the open problem.

Theorem 1.1 (Lower envelope over W_{ij} for $n \geq 3$)**.** *Suppose $n \geq 3$, $a \in \mathbb{R}^n_{++}$, $0 < p < q$, $0 \leq \ell < u < \infty$, and $i \neq j$. Then*

$$\mathcal{E}^-_{\ell,u} = \{(x,z) \in \mathbb{R}^n_+ \times \mathbb{R} : px_i \leq x_j \leq qx_i,\ f(x) \geq \ell,\ z \geq \ell\}. \tag{7}$$

Equivalently, the lower convex envelope of f on $X_{\ell,u} \cap W_{ij}$ is

$$\operatorname{vex}_{X_{\ell,u}\cap W_{ij}} f(x) = \begin{cases} \ell, & x \in W_{ij},\ f(x) \geq \ell, \\ +\infty, & \textit{otherwise}. \end{cases} \tag{8}$$

The theorem is stronger than a description of a single valid underestimator. It states that every point of the lower epigraph hull can be generated from level-ℓ graph points and vertical rays, and that every convex underestimator valid on $X_{\ell,u} \cap W_{ij}$ is bounded above by ℓ on the whole convexified domain. Consequently, within the relaxation determined solely by $T_{\ell,u}$ and W_{ij}, no convex lower-side inequality–including nonlinear lower cuts, perspective strengthenings, or additional two-variable convex underestimators–can improve $z \geq \ell$ once $n \geq 3$.

The proof rests on a level-set identity that appears to be absent from the preceding literature on monomial convexification. For every $\xi \geq 0$,

$$\operatorname{conv}\{x \in W_{ij} : f(x) = \xi\} = \{x \in W_{ij} : f(x) \geq \xi\}. \tag{9}$$

The inclusion "$\subseteq$" follows from convexity of monomial superlevel sets. For the reverse inclusion, take $x \in W_{ij}$ with $f(x) > \xi$. Because $n \geq 3$, choose $h \notin \{i,j\}$ and move along the line

$$\begin{aligned} x_i(t) &= x_i - t, \\ x_j(t) &= \frac{x_j}{x_i}(x_i - t), \\ x_h(t) &= x_h + t. \end{aligned} \tag{10}$$

with all other coordinates fixed. For $t < x_i$, the ratio $x_j(t)/x_i(t)$ is constant and belongs to $[p,q]$; at the endpoint $t = x_i$ both constrained coordinates are zero, and the cone inequalities still hold because $x_j(t) = rx_i(t)$ with $r = x_j/x_i \in [p,q]$. At both ends of the feasible interval the monomial is zero, while at $t = 0$ it is $f(x) > \xi$. Continuity gives two points of level ξ on opposite sides of x, and x is their convex combination. This two-point construction is the whole source of the dimensional dichotomy.

The relevance of the result to global optimization is direct. Convex envelopes of multilinear, polynomial, and more general factorable terms are central in deterministic nonconvex optimization.[2–10] Classical factorable programming decomposes complex expressions into elementary terms and then convexifies the corresponding graph, epigraph, or hypograph pieces before embedding them in a branch-and-bound relaxation.[11–17] In that workflow a closed-form envelope is valuable for two reasons. First, it avoids auxiliary reformulations that may introduce relaxation gaps. Second, it gives a separation target whose validity is independent of a particular solver implementation.

Broader recent work in nonlinear analysis, computational intelligence, and complex analysis also illustrates the continued role of nonlinear structure, level-set reasoning, stability, and optimization-inspired techniques across applied mathematics.[18–24] These references are included for contextual breadth; the direct predecessors of the present envelope theorem remain the convexification and deterministic global-optimization literature cited above.

Monomial functions also arise naturally in geometric programming, positive-system design, circuit optimization, aircraft design, and posynomial optimization.[25–33] These applications usually exploit logarithmic transformations or conic representations, but branch-and-bound algorithms still require tight relaxations when discrete decisions, signomial terms, or bounded auxiliary products appear. The two-variable cone $px_i \leq x_j \leq qx_i$ is especially relevant to branching and cutting strategies because it restricts a ratio rather than an absolute coordinate interval. Belotti's work shows that this ratio restriction preserves a tractable upper envelope and gives a nontrivial lower envelope in two dimensions. The present paper shows that, as soon as a third positive coordinate is available, the lower side has no residual curvature: it is exactly the level lower bound $z \geq \ell$ on the convexified projection. Combining (7) with Belotti's upper envelope gives the complete graph hull for every $n \geq 3$. The lower envelope is independent of the upper value bound u, but the full graph hull is not; its upper endpoint still depends on u.

The contribution is not just the observation that $z \geq \ell$ is valid. That inequality is immediate from the definition of $T_{\ell,u}$. The substantive point is maximality: after convexifying the projection, no convex function can lie above the constant ℓ while remaining below the monomial on the original bounded set. This is a strong statement because $\mathrm{conv}(T_{\ell,u})$ is typically unbounded even when $T_{\ell,u}$ is cut by the upper value bound $f(x) \leq u$. The proof explains this apparent paradox. The upper value bound disappears from the lower epigraph because every point of the superlevel set S_ℓ can be reconstructed from two level-ℓ points. Hence the lower epigraph hull is generated by the lowest graph layer, not by the full annular set $\ell \leq f(x) \leq u$.

The paper also records algorithmic consequences that are useful for implementation. A point in the convexified projection has an explicit two-point certificate; a point outside the projection has either a linear cone violation, a nonnegativity violation, or a monomial superlevel violation that can be separated by a logarithmic gradient cut when the point is strictly positive. These statements connect the exact geometry to practical relaxation design. Related themes appear in bounds tightening, volume-based comparison, and branching studies for nonconvex mixed-integer optimization.[34–38] The convex-analytic tools used here are standard–convex hulls, projections, supporting hyperplanes, and hypograph/epigraph calculus–but their combination with the compensating-coordinate path is specific to the cone W_{ij}.[39–42] The numerical section follows the tradition of computational validation for relaxation geometry and mixed-integer optimization, while keeping the computations reproducible and secondary to the proof.[43–45]

Section 2 presents notation, the two-point proof method, and the reproducible computational protocol. Section 3 gives the exact lower envelope, the complete bounded graph hull, the dimension-sharp dichotomy, and numerical illustrations. Section 4 discusses constructive decomposition, separation, persistence under additional restrictions, and limitations. The final section summarizes the contribution.

2. Methods

The proof method is geometric rather than algorithmic. It identifies a level set whose convex hull is already the full monomial superlevel set inside the two-variable cone. This section fixes the notation, proves the convexity facts needed later, develops the compensating-coordinate construction, and records the computational protocol used for the numerical illustrations in Section 3.4.

2.1. Notation and convexity preliminaries

Throughout the paper,

$$n \geq 3, \qquad a = (a_1, \ldots, a_n) \in \mathbb{R}^n_{++}, \qquad \beta := \sum_{k=1}^{n} a_k, \tag{11}$$

unless a result explicitly states otherwise. For real exponents on the boundary of $\mathbb{R}^n_+$, we use the standard convention

$$0^\alpha = 0, \qquad \alpha > 0. \tag{12}$$

The index set is $N := \{1, \ldots, n\}$, and $i, j \in N$ are distinct. We use W_{ij} for the cone (3), $X_{\ell,u}$ for (2), and

$$T_{\ell,u} := X_{\ell,u} \cap W_{ij}. \tag{13}$$

For a set $S \subseteq \mathbb{R}^n_+$, the restricted epigraph and hypograph are

$$\mathrm{epi}(f, S) := \{(x, z) \in S \times \mathbb{R} : z \geq f(x)\}, \tag{14}$$

$$\mathrm{hyp}(f, S) := \{(x, z) \in S \times \mathbb{R} : z \leq f(x)\}. \tag{15}$$

The graph is

$$\mathrm{gr}(f, S) := \{(x, z) \in S \times \mathbb{R} : z = f(x)\}. \tag{16}$$

The lower and upper envelope sets are

$$\mathcal{E}^-(f, S) := \mathrm{conv}(\mathrm{epi}(f, S)), \tag{17}$$

$$\mathcal{E}^+(f, S) := \mathrm{conv}(\mathrm{hyp}(f, S)). \tag{18}$$

When $S = T_{\ell,u}$, these coincide with $\mathcal{E}^-_{\ell,u}$ and $\mathcal{E}^+_{\ell,u}$ in (5)–(6).

We shall repeatedly use the following notation for monomial level and superlevel sets inside W_{ij}:

$$L_\xi := \{x \in W_{ij} : f(x) = \xi\}, \tag{19}$$

$$S_\xi := \{x \in W_{ij} : f(x) \geq \xi\}, \tag{20}$$

where $\xi \geq 0$.

Notice that

$$T_{\ell,u} = S_\ell \cap \{x \in \mathbb{R}^n_+ : f(x) \leq u\}. \tag{21}$$

The lower envelope will depend on u only through the requirement that the level $f = \ell$ belongs to $T_{\ell,u}$.

Lemma 2.1 (Convexity of monomial superlevel sets)**.** *For every $\xi \geq 0$, the set*

$$\{x \in \mathbb{R}^n_+ : f(x) \geq \xi\} \tag{22}$$

is convex. Consequently S_ξ is convex.

Proof. The case $\xi = 0$ is immediate because (22) equals $\mathbb{R}^n_+$. Let $\xi > 0$ and let $x, y \in \mathbb{R}^n_+$ satisfy $f(x) \geq \xi$ and $f(y) \geq \xi$. Then $x, y \in \mathbb{R}^n_{++}$. For $\lambda \in [0,1]$, coordinatewise concavity of the logarithm gives

$$\log(\lambda x_k + (1-\lambda)y_k) \geq \lambda \log x_k + (1-\lambda)\log y_k, \quad k \in N. \tag{23}$$

Multiplying by $a_k > 0$ and summing yields

$$\begin{aligned}\log f(\lambda x + (1-\lambda)y) &= \sum_{k=1}^{n} a_k \log(\lambda x_k + (1-\lambda)y_k)\\ &\geq \lambda \sum_{k=1}^{n} a_k \log x_k\\ &\quad + (1-\lambda)\sum_{k=1}^{n} a_k \log y_k\\ &= \lambda \log f(x) + (1-\lambda)\log f(y)\\ &\geq \log \xi.\end{aligned} \tag{24}$$

Thus $f(\lambda x + (1-\lambda)y) \geq \xi$. Intersecting with the convex cone W_{ij} preserves convexity. $\square$

Remark 2.2 (Boundary convention for the logarithmic argument). For $\xi > 0$, the superlevel condition $f(x) \geq \xi$ forces every coordinate of x to be strictly positive because all exponents are positive. Thus the logarithmic proof of Lemma 2.1 is applied only in $\mathbb{R}^n_{++}$. Boundary points with zero coordinates occur only when $\xi = 0$, or as endpoint limits in the path construction below. The convention $0^\alpha = 0$ and continuity of f on $\mathbb{R}^n_+$ justify these endpoint evaluations.

Remark 2.3 (Convexity is independent of homogeneity). Lemma 2.1 uses only $a_k > 0$. The value of $\beta = \sum_k a_k$ plays no role in the lower envelope. The parameter β enters only in the upper envelope: when $\beta \leq 1$, the monomial is concave on $\mathbb{R}^n_+$, while for $\beta > 1$ the upper envelope is described by the corresponding secant form rather than by concavity of f itself. The concavity assertion follows by setting $a_0 := 1 - \beta \geq 0$: the map $(x,t) \mapsto \prod_{k=1}^n x_k^{a_k} t^{a_0}$ is a weighted geometric mean with nonnegative weights summing to one, and evaluating it at the fixed value $t = 1$ gives concavity of f on $\mathbb{R}^n_+$.

The next elementary fact is useful when passing from epigraphs to scalar envelopes.

Lemma 2.4 (Projection of a convex epigraph hull). *Let $S \subseteq \mathbb{R}^n_+$ and $f : S \to \mathbb{R}$. Then*

$$\operatorname{proj}_x\big(\operatorname{conv}(\operatorname{epi}(f,S))\big) = \operatorname{conv}(S). \tag{25}$$

Moreover, if $m \leq f(x)$ for every $x \in S$, then every $(x,z) \in \operatorname{conv}(\operatorname{epi}(f,S))$ satisfies $z \geq m$.

Proof. The inclusion "$\subseteq$" in (25) follows by projecting a convex combination of epigraph points. For "$\supseteq$", write $x = \sum_{r=1}^R \lambda_r x^r$ with $x^r \in S$, $\lambda_r \geq 0$, and $\sum_r \lambda_r = 1$. Then $(x, \sum_r \lambda_r f(x^r))$ belongs to $\operatorname{conv}(\operatorname{epi}(f,S))$. The lower bound on z follows by taking convex combinations of numbers at least m. $\square$

2.2. A level-set convexification identity

This section proves the identity that drives the lower envelope. It is worth stating first without the upper bound u, since the upper bound disappears from the lower epigraph after convexification.

Theorem 2.5 (Two-point convexification of monomial levels). *Let $n \geq 3$, $a \in \mathbb{R}^n_{++}$, $i \neq j$, and $0 < p < q$. For every $\xi \geq 0$,*

$$\operatorname{conv}(L_\xi) = S_\xi. \tag{26}$$

More precisely, every $x \in S_\xi$ is either in L_ξ or is a convex combination of two points of L_ξ.

The proof treats the zero and positive levels separately at the only place where the distinction matters: for $\xi > 0$ the two certificate points are interior roots found by continuity, whereas for $\xi = 0$ they are the two zero-product endpoints of the same affine path.

Proof. By Lemma 2.1, S_ξ is convex. Since $L_\xi \subseteq S_\xi$, we immediately have

$$\operatorname{conv}(L_\xi) \subseteq S_\xi. \tag{27}$$

It remains to prove the reverse inclusion.

Fix $x \in S_\xi$. If $f(x) = \xi$, then $x \in L_\xi$ and there is nothing to prove. Hence assume

$$f(x) > \xi. \tag{28}$$

Then $f(x) > 0$, so every coordinate of x is strictly positive. In particular $x_i > 0$, and

$$r := \frac{x_j}{x_i} \in [p,q]. \tag{29}$$

Because $n \geq 3$, choose an index

$$h \in N \setminus \{i,j\}. \tag{30}$$

For $t \in [-x_h, x_i]$, define $x(t) \in \mathbb{R}^n_+$ by

$$x_i(t) := x_i - t, \tag{31}$$
$$x_j(t) := r(x_i - t), \tag{32}$$
$$x_h(t) := x_h + t, \tag{33}$$
$$x_k(t) := x_k, \qquad k \in N \setminus \{i,j,h\}. \tag{34}$$

The interval $[-x_h, x_i]$ is chosen exactly so that the two moving nonnegative quantities $x_i(t)$ and $x_h(t)$ remain nonnegative. Moreover,

$$x_j(t) = r x_i(t), \qquad r \in [p,q], \tag{35}$$

and therefore

$$x(t) \in W_{ij}, \qquad -x_h \leq t \leq x_i. \tag{36}$$

The map $t \mapsto x(t)$ is affine and satisfies $x(0) = x$.

Along this line the monomial is the univariate continuous function

$$\begin{aligned}\phi(t) &:= f(x(t)) \\ &= (x_i - t)^{a_i}\big(r(x_i - t)\big)^{a_j}(x_h + t)^{a_h} \\ &\quad \times \prod_{k\in N\setminus\{i,j,h\}} x_k^{a_k} \\ &= r^{a_j}\,(x_i - t)^{a_i+a_j}\,(x_h + t)^{a_h} \\ &\quad \times \prod_{k\in N\setminus\{i,j,h\}} x_k^{a_k}.\end{aligned} \tag{37}$$

At the two endpoints,

$$\phi(-x_h) = 0, \qquad \phi(x_i) = 0, \tag{38}$$

whereas

$$\phi(0) = f(x) > \xi. \tag{39}$$

If $\xi > 0$, the intermediate value theorem gives points

$$\begin{gathered} t^- \in (-x_h, 0), \qquad t^+ \in (0, x_i), \\ \phi(t^-) = \phi(t^+) = \xi. \end{gathered} \tag{40}$$

If $\xi = 0$, set instead

$$t^- := -x_h, \qquad t^+ := x_i, \tag{41}$$

which again gives $t^- < 0 < t^+$ and $\phi(t^-) = \phi(t^+) = \xi$.

Define

$$\lambda := \frac{t^+}{t^+ - t^-} \in (0,1). \tag{42}$$

Then

$$\lambda t^- + (1-\lambda)t^+ = 0. \tag{43}$$

Using the affine definition (31)–(34), we obtain

$$\lambda x(t^-) + (1-\lambda)x(t^+) = x(0) = x. \tag{44}$$

Because $x(t^-), x(t^+) \in W_{ij}$ and $f(x(t^-)) = f(x(t^+)) = \xi$, both points belong to L_ξ. Thus $x \in \operatorname{conv}(L_\xi)$. This proves $S_\xi \subseteq \operatorname{conv}(L_\xi)$, and hence (26). The same argument gives the asserted two-point representation. □

Remark 2.6 (The compensating coordinate). The proof uses only one coordinate $h \notin \{i,j\}$. The pair (x_i, x_j) moves along the ray relation $x_j(t) = rx_i(t)$ inside the two-variable cone, with the quotient $x_j(t)/x_i(t)$ interpreted only when $x_i(t) > 0$, while x_h absorbs the mass displaced from x_i. The remaining coordinates are frozen. Thus the proof is local in the sense that no balancing across all n variables is needed; the extra dimension is used solely to make the line segment have two zero-product endpoints.

Corollary 2.7 (Convex hull of the bounded monomial slice)**.** *For $n \geq 3$,*

$$\begin{aligned}\operatorname{conv}(T_{\ell,u}) = S_\ell = \{x \in \mathbb{R}^n_+ : px_i \leq x_j \leq qx_i,\\ f(x) \geq \ell\}.\end{aligned} \tag{45}$$

The identity is independent of u as long as $u \geq \ell$.

Proof. Since $T_{\ell,u} \subseteq S_\ell$ and S_ℓ is convex, we have

$$\operatorname{conv}(T_{\ell,u}) \subseteq S_\ell. \tag{46}$$

On the other hand, $L_\ell \subseteq T_{\ell,u}$ because every point of L_ℓ satisfies $\ell \leq f(x) = \ell \leq u$. Therefore, by Theorem 2.5,

$$S_\ell = \operatorname{conv}(L_\ell) \subseteq \operatorname{conv}(T_{\ell,u}). \tag{47}$$

Combining (46) and (47) gives (45). □

Corollary 2.8 (Two-point representation for the projection)**.** *For every $x \in \operatorname{conv}(T_{\ell,u})$ there exist $y^-, y^+ \in T_{\ell,u}$ and $\lambda \in [0,1]$ such that*

$$f(y^-) = f(y^+) = \ell, \qquad x = \lambda y^- + (1-\lambda)y^+. \tag{48}$$

If $f(x) = \ell$, one may choose $y^- = y^+ = x$.

Proof. By Corollary 2.7, $x \in S_\ell$. Apply the constructive statement in Theorem 2.5 with $\xi = \ell$. □

2.3. Computational protocol

The analytical results below do not rely on numerical evidence. Nevertheless, numerical experiments are useful for three purposes: they expose the geometry of the two-point construction, they test the conditioning of the certificate-generation procedure, and they provide reproducible figures for readers who want to inspect the envelope on representative slices. All computations in Section 3.4 use synthetic instances generated by the supplied Python script `numerical_experiments.py`. No external data set is used.

For a sampled point $x \in S_\ell$ with $f(x) > \ell$, the script chooses the first index $h \notin \{i,j\}$, fixes $r = x_j/x_i$, and forms the affine path (31)–(34). The two roots $t^- < 0 < t^+$ of $f(x(t)) = \ell$ are found by bracketed bisection in logarithmic value space. For $\ell > 0$, the implementation solves

$$g(t) := \sum_{k=1}^{n} a_k \log x_k(t) - \log \ell = 0 \tag{49}$$

on the open intervals $(-x_h, 0)$ and $(0, x_i)$. The endpoint values are understood as the one-sided limits $g(-x_h^+) = -\infty$ and $g(x_i^-) = -\infty$; numerically, the brackets are initialized at interior points so that no logarithm is evaluated at a zero coordinate. This avoids loss of precision when the dimension or the homogeneity degree is large. The certificate then uses $y^- = x(t^-)$, $y^+ = x(t^+)$, and $\lambda = t^+/(t^+ - t^-)$. The reported stress tests used a bisection tolerance of 10^{-13} for the two certificate roots, with a cap of 140 bisection iterations. The auxiliary root routine stops when the logarithmic residual or bracket length meets this tolerance, and the endpoint level residual is then reported independently rather than forced to zero. The script reports the relative reconstruction residual

$$\frac{\|\lambda y^- + (1-\lambda)y^+ - x\|_2}{\max\{1, \|x\|_2\}} \tag{50}$$

and the maximum relative level residual at the two endpoints. The implementation also checks nonnegativity and the two cone inequalities. Figures are generated at 600 dpi and are included as PNG files in the source package.

The sampling scheme is deliberately simple. For each regime, the script first draws positive coordinates on a logarithmic scale, then enforces a uniformly sampled ratio $r \in [p, q]$ by setting $x_j = rx_i$. If the resulting point does not satisfy $f(x) > \ell$, the whole vector is scaled by a positive factor until the superlevel condition is strict. This preserves membership in W_{ij} because the cone is homogeneous. The procedure is not meant to mimic a solver's incumbent distribution; it is meant to probe the certificate over points with different scales, ratios, dimensions, and homogeneity degrees. The table of residuals therefore tests the algebraic construction rather than a statistical hypothesis.

3. Results

3.1. The lower envelope

We now prove the exact lower epigraph hull. The proof is short because the entire geometric content is already contained in Theorem 2.5.

Theorem 3.1 (Exact lower epigraph hull)**.** *Let $n \geq 3$, $a \in \mathbb{R}^n_{++}$, $i \neq j$, $0 < p < q$, and $0 \leq \ell < u < \infty$. Then*

$$\begin{aligned}\operatorname{conv}(\operatorname{epi}(f, T_{\ell,u})) = \{(x,z) \in \mathbb{R}^n_+ \times \mathbb{R} : px_i \leq x_j \leq qx_i,\\ f(x) \geq \ell,\ z \geq \ell\}.\end{aligned} \tag{51}$$

Here the product notation means

$$\begin{aligned}S_\ell \times [\ell, \infty) = \{(x,z) \in \mathbb{R}^n_+ \times \mathbb{R} : px_i \leq x_j \leq qx_i,\\ f(x) \geq \ell,\ z \geq \ell\}.\end{aligned} \tag{52}$$

Proof. Let $(x, z) \in \operatorname{conv}(\operatorname{epi}(f, T_{\ell,u}))$. By Lemma 2.4 and Corollary 2.7,

$$x \in \operatorname{conv}(T_{\ell,u}) = S_\ell. \tag{53}$$

Moreover $f(y) \geq \ell$ for every $y \in T_{\ell,u}$, so every point of $\operatorname{epi}(f, T_{\ell,u})$ has vertical coordinate at least ℓ. Convex combinations preserve this lower bound, hence $z \geq \ell$. Thus

$$\operatorname{conv}(\operatorname{epi}(f, T_{\ell,u})) \subseteq S_\ell \times [\ell, \infty). \tag{54}$$

Conversely, fix $(x, z) \in S_\ell \times [\ell, \infty)$. By Corollary 2.8, choose $y^-, y^+ \in T_{\ell,u}$ and $\lambda \in [0, 1]$ satisfying

$$f(y^-) = f(y^+) = \ell, \qquad x = \lambda y^- + (1-\lambda)y^+. \tag{55}$$

Since $z \geq \ell = f(y^-) = f(y^+)$, both (y^-, z) and (y^+, z) belong to $\operatorname{epi}(f, T_{\ell,u})$. Therefore

$$\begin{aligned}(x, z) &= \lambda(y^-, z) + (1-\lambda)(y^+, z)\\ &\in \operatorname{conv}(\operatorname{epi}(f, T_{\ell,u})).\end{aligned} \tag{56}$$

This proves the reverse inclusion and hence (51). □

Several features of Theorem 3.1 deserve emphasis. First, the set on the right side of (51) is closed and convex. Convexity follows from Lemma 2.1, the linearity of the cone inequalities, and the half-line constraint $z \geq \ell$. Thus no additional closure operation is hidden in the notation. Second, the upper value bound u has disappeared completely. This is not because u is irrelevant to the original graph; it remains essential for the upper envelope and for the graph hull. The upper value bound disappears only from the lower epigraph hull because the level-ℓ slice is already rich enough to generate every point of the convexified projection. Third, the proof is constructive with two points rather than a generic dimension-dependent convex combination. This is stronger than a dimension-dependent existence result and is important for numerical certification because only one scalar root is needed on each side of the sampled point.

The theorem also identifies the exact obstruction to convex lower-side strengthening. Any affine inequality valid for the lower epigraph hull, and more generally any lower convex estimator g satisfying $g \leq f$ on $T_{\ell,u}$, must be valid at all level-ℓ points. Since those level points convexify to form S_ℓ, convexity forces such an estimator to satisfy $g \leq \ell$ on the entire convexified projection. A curved lower convex estimator can therefore be valid on the original bounded set only if it lies below ℓ somewhere on S_ℓ; it cannot dominate the constant estimator. This explains why standard strengthening mechanisms such as perspective cuts or additional monomial underestimators do not improve the lower side unless they use information not contained in $T_{\ell,u}$.

Theorem 3.1 gives a scalar form of the lower convex envelope. Define the extended-real lower convex envelope by

$$\begin{aligned}\operatorname{vex}_{T_{\ell,u}} f(x) := \inf\{z \in \mathbb{R} :\\ (x, z) \in \operatorname{conv}(\operatorname{epi}(f, T_{\ell,u}))\}.\end{aligned} \tag{57}$$

Then (51) immediately yields the following formula.

Corollary 3.2 (Flat lower convex envelope)**.** *For $n \geq 3$,*

$$\operatorname{vex}_{T_{\ell,u}} f(x) = \begin{cases} \ell, & \substack{x\in\mathbb{R}^n_+,\ px_i\le x_j\le qx_i,\\ f(x)\ge\ell,} \\ +\infty, & \textit{otherwise.} \end{cases} \tag{58}$$

Proof. The infimum in (57) is ℓ exactly for $x \in S_\ell$ and is over the empty set otherwise. ☐

The next theorem records a sharp minimality property. It rules out any stronger finite-valued convex underestimator on S_ℓ, and equivalently any convex epigraph-side strengthening based only on $T_{\ell,u}$ that could improve $z \geq \ell$ after projecting onto $\operatorname{conv}(T_{\ell,u})$.

Theorem 3.3 (No stronger lower convex underestimator)**.** *Let $g : S_\ell \to \mathbb{R}$ be a convex function satisfying*

$$g(x) \leq f(x), \qquad x \in T_{\ell,u}. \tag{59}$$

Then

$$g(x) \leq \ell, \qquad x \in S_\ell. \tag{60}$$

Consequently the constant function ℓ is the pointwise largest finite-valued convex lower underestimator on the convexified domain S_ℓ.

Proof. Fix $x \in S_\ell$. By Corollary 2.8, write

$$\begin{gathered} x = \lambda y^- + (1-\lambda)y^+, \\ y^-, y^+ \in T_{\ell,u}, \qquad f(y^-) = f(y^+) = \ell. \end{gathered} \tag{61}$$

Using convexity of g and validity on $T_{\ell,u}$,

$$\begin{aligned} g(x) &\leq \lambda g(y^-) + (1-\lambda)g(y^+) \\ &\leq \lambda f(y^-) + (1-\lambda)f(y^+) \\ &= \lambda\ell + (1-\lambda)\ell = \ell. \end{aligned} \tag{62}$$

The constant function $g \equiv \ell$ is itself convex and valid on $T_{\ell,u}$, so the bound is attained. ☐

Remark 3.4 (The role of the upper bound u). The lower envelope is independent of u. The upper bound $f(x) \leq u$ can be removed, tightened, or replaced by any restriction whose feasible set remains sandwiched between the level set L_ℓ and the superlevel set S_ℓ. More precisely, if $Y \subseteq W_{ij}$ satisfies $L_\ell \subseteq Y \subseteq S_\ell$, then

$$\operatorname{conv}(\operatorname{epi}(f, Y)) = S_\ell \times [\ell, \infty). \tag{63}$$

In particular this holds for $Y = T_{\ell,u}$ for every $u \geq \ell$.

3.2. The full graph hull for $n \geq 3$

This section combines Theorem 3.1 with the upper envelope established in.[1] Since the cited upper-envelope theorem is stated for a positive lower bound, we record it in that form first and then prove the limiting $\ell = 0$ upper-envelope formulas needed for the graph-hull statements below.

Let

$$\begin{aligned} \mathcal{G}_{\ell,u} = \operatorname{gr}(f, T_{\ell,u}) = \{(x,z) : x \in W_{ij},\ \ell \leq f(x) \leq u, \\ z = f(x)\}. \end{aligned} \tag{64}$$

For $0 < \ell < u$ and $\beta > 1$, define

$$z_0 := \frac{u^{1/\beta}\ell - \ell^{1/\beta}u}{u^{1/\beta} - \ell^{1/\beta}}, \tag{65}$$

$$\gamma := \left(\frac{u-\ell}{u^{1/\beta} - \ell^{1/\beta}}\right)^\beta. \tag{66}$$

The two constants in (65)–(66) are the standard secant constants for the homogeneous monomial upper envelope in the case $\beta > 1$. For later use, note that $z_0 < 0 < \ell$ when $0 < \ell < u$ and $\beta > 1$. Indeed, with $s := u^{1/\beta}$ and $t := \ell^{1/\beta}$, one has $s > t > 0$ and

$$z_0 = \frac{st^\beta - ts^\beta}{s-t} = \frac{st\left(t^{\beta-1} - s^{\beta-1}\right)}{s-t} < 0. \tag{67}$$

Theorem 3.5 (Known upper envelope for $0 < \ell < u$; Belotti)**.** *Assume $n \geq 3$, $a \in \mathbb{R}^n_{++}$, $i \neq j$, $0 < p < q$, and $0 < \ell < u < \infty$. The upper hypograph hull over $T_{\ell,u}$ is as follows. If $\beta > 1$, then*

$$\begin{aligned} \operatorname{conv}(\operatorname{hyp}(f, T_{\ell,u})) = \{(x,z) : x \in W_{ij},\ f(x) \geq \ell, \\ z \leq u, \\ z \leq z_0 + \gamma^{1/\beta} f(x)^{1/\beta}\}. \end{aligned} \tag{68}$$

If $\beta \leq 1$, then

$$\begin{aligned} \operatorname{conv}(\operatorname{hyp}(f, T_{\ell,u})) = \{(x,z) : x \in W_{ij},\ f(x) \geq \ell, \\ z \leq u,\ z \leq f(x)\}. \end{aligned} \tag{69}$$

Remark 3.6 (Power form and complete hypographs). For $\beta > 1$ and $0 < \ell < u$, the inequality

$$(z - z_0)^\beta \leq \gamma f(x) \tag{70}$$

is equivalent to the last inequality in (68) only on the region where $z - z_0 \geq 0$. In the graph-hull statements below this causes no ambiguity, because the lower envelope contributes $z \geq \ell$ and (67) gives $z_0 < \ell$. For the complete hypograph hull itself, however, (68) is the unambiguous formulation, especially when β is not an integer.

Proposition 3.7 (Upper envelope at $\ell = 0$)**.** *Assume $n \geq 3$ and $0 < u < \infty$. If $\beta > 1$, then*

$$\begin{aligned} \operatorname{conv}(\operatorname{hyp}(f, T_{0,u})) = \{(x,z) : x \in W_{ij},\ z \leq u, \\ z \leq u^{(\beta-1)/\beta} f(x)^{1/\beta}\}. \end{aligned} \tag{71}$$

If $\beta \leq 1$, then

$$\begin{aligned} \operatorname{conv}(\operatorname{hyp}(f, T_{0,u})) = \{(x,z) : x \in W_{ij},\ z \leq u, \\ z \leq f(x)\}. \end{aligned} \tag{72}$$

Proof. The hypograph hull is downward closed in the z coordinate, so it is enough to realize the maximal admissible vertical coordinate at each x.

First suppose $\beta > 1$. Set

$$F(x) := f(x)^{1/\beta}, \qquad \alpha := u^{1/\beta}. \tag{73}$$

The function F is the weighted geometric mean with weights a_k/β, hence is concave and positively homogeneous of degree one on $\mathbb{R}^n_+$. For every $(y, w) \in \operatorname{hyp}(f, T_{0,u})$,

$$w \le f(y) = F(y)^\beta \le \alpha^{\beta-1}F(y), \qquad w \le u. \tag{74}$$

Taking convex combinations and using concavity of F proves the inclusion "$\subseteq$" in (71).

For the reverse inclusion, fix $x \in W_{ij}$. If $F(x) = 0$, then $x \in T_{0,u}$ and $(x, 0) \in \operatorname{hyp}(f, T_{0,u})$. If $0 < F(x) < \alpha$, set

$$y := \frac{\alpha}{F(x)}x, \qquad \lambda := \frac{F(x)}{\alpha}. \tag{75}$$

Then $y \in W_{ij}$, $f(y) = u$, and

$$(x, \alpha^{\beta-1}F(x)) = \lambda(y, u) + (1 - \lambda)(0, 0), \tag{76}$$

where both lifted points on the right belong to $\operatorname{hyp}(f, T_{0,u})$. If $F(x) \ge \alpha$, then $f(x) \ge u$, so Theorem 2.5 with $\xi = u$ gives $x \in \operatorname{conv}(L_u)$. Hence x is a convex combination of points $y^r \in W_{ij}$ with $f(y^r) = u$, and therefore (x, u) is the same convex combination of the graph points (y^r, u). This proves (71).

Now suppose $\beta \le 1$. The monomial f is concave on $\mathbb{R}^n_+$: with $a_0 := 1 - \beta \ge 0$, the function $(x, t) \mapsto \prod_{k=1}^n x_k^{a_k} t^{a_0}$ is a weighted geometric mean with weights summing to one, and restricting it to $t = 1$ gives f. Thus every convex combination of points in $\operatorname{hyp}(f, T_{0,u})$ satisfies $z \le f(x)$, and the bound $z \le u$ is preserved by convex combinations; this proves the inclusion "$\subseteq$" in (72). Conversely, if $x \in W_{ij}$ and $f(x) \le u$, then $(x, f(x)) \in \operatorname{hyp}(f, T_{0,u})$. If $f(x) > u$, then Theorem 2.5 with $\xi = u$ gives $x \in \operatorname{conv}(L_u)$, and hence (x, u) is a convex combination of level-u graph points. Downward closedness gives all smaller z values. This proves (72). $\square$

For completeness, we first state a standard vertical-fiber fact for scalar graph hulls.

Lemma 3.8 (Intersection of lower and upper envelope hulls)**.** *Let $S \subseteq \mathbb{R}^n_+$ and $f : S \to \mathbb{R}$. Then*

$$\operatorname{conv}(\operatorname{gr}(f, S)) = \operatorname{conv}(\operatorname{epi}(f, S)) \cap \operatorname{conv}(\operatorname{hyp}(f, S)). \tag{77}$$

In particular, the graph hull is obtained by imposing the lower and upper envelope inequalities simultaneously.

Proof. Set $C := \operatorname{conv}(\operatorname{gr}(f, S))$. Since

$$\begin{aligned} \operatorname{epi}(f, S) &= \operatorname{gr}(f, S) + (\{0\}^n \times \mathbb{R}_+), \\ \operatorname{hyp}(f, S) &= \operatorname{gr}(f, S) + (\{0\}^n \times \mathbb{R}_-). \end{aligned} \tag{78}$$

and the two vertical rays are convex cones, we have

$$\begin{aligned} \operatorname{conv}(\operatorname{epi}(f, S)) &= C + (\{0\}^n \times \mathbb{R}_+), \\ \operatorname{conv}(\operatorname{hyp}(f, S)) &= C + (\{0\}^n \times \mathbb{R}_-). \end{aligned} \tag{79}$$

The inclusion $C \subseteq \operatorname{conv}(\operatorname{epi}(f, S)) \cap \operatorname{conv}(\operatorname{hyp}(f, S))$ is immediate.

Conversely, let (x, z) belong to the intersection. By (79), there exist $z^-, z^+ \in \mathbb{R}$ such that

$$(x, z^-) \in C, \qquad (x, z^+) \in C, \qquad z^- \le z \le z^+. \tag{80}$$

If $z^- = z^+$ there is nothing to prove. Otherwise, with

$$\lambda := \frac{z^+ - z}{z^+ - z^-} \in [0, 1], \tag{81}$$

convexity of C gives

$$(x, z) = \lambda(x, z^-) + (1 - \lambda)(x, z^+) \in C. \tag{82}$$

Thus the reverse inclusion holds. $\square$

Theorem 3.9 (Convex hull of the bounded graph, $\beta > 1$)**.** *Assume $n \ge 3$, $0 \le \ell < u < \infty$, and $\beta > 1$. If $0 < \ell$, then*

$$\begin{aligned} \operatorname{conv}(\mathcal{G}_{\ell,u}) = \{(x, z) \in \mathbb{R}^n_+ \times \mathbb{R} : {} & px_i \le x_j \le qx_i, \\ & f(x) \ge \ell, \\ & \ell \le z \le u, \\ & (z - z_0)^\beta \le \gamma f(x)\}. \end{aligned} \tag{83}$$

where z_0 and γ are defined by (65)–(66)*. If $\ell = 0$, then*

$$\begin{aligned} \operatorname{conv}(\mathcal{G}_{\ell,u}) = \{(x, z) \in \mathbb{R}^n_+ \times \mathbb{R} : {} & px_i \le x_j \le qx_i, \\ & 0 \le z \le u, \\ & z^\beta \le u^{\beta-1} f(x)\}. \end{aligned} \tag{84}$$

Proof. By Theorem 3.1, the lower envelope contributes exactly

$$\begin{aligned} & x \in W_{ij}, \qquad f(x) \ge \ell, \\ & z \ge \ell. \end{aligned} \tag{85}$$

If $0 < \ell$, Theorem 3.5 contributes

$$\begin{aligned} & x \in W_{ij}, \qquad f(x) \ge \ell, \\ & z \le u, \\ & z \le z_0 + \gamma^{1/\beta} f(x)^{1/\beta}. \end{aligned} \tag{86}$$

Because $z_0 < \ell$ by (67), after intersecting with $z \ge \ell$ the last inequality in (86) is equivalent to

$$(z - z_0)^\beta \le \gamma f(x). \tag{87}$$

Lemma 3.8 gives (83).

If $\ell = 0$, Theorem 3.1 gives $x \in W_{ij}$ and $z \ge 0$, while Proposition 3.7 gives

$$\begin{aligned} & z \le u, \\ & z \le u^{(\beta-1)/\beta} f(x)^{1/\beta}. \end{aligned} \tag{88}$$

On the region $z \geq 0$, the second inequality in (88) is equivalent to

$$z^\beta \leq u^{\beta-1} f(x). \tag{89}$$

Applying Lemma 3.8 proves (84). $\square$

Remark 3.10 (Real powers and nonnegative bases). All real powers in (83) and (84) are understood on their nonnegative bases. In (83), the constraints give $z \geq \ell$ and (67) gives $z_0 < \ell$, so $z - z_0 > 0$. In (84), the constraint $z \geq 0$ ensures that z^β is well defined. The monomial powers use the boundary convention (12).

Theorem 3.11 (Convex hull of the bounded graph, $\beta \leq 1$)**.** *Assume $n \geq 3$, $0 \leq \ell < u < \infty$, and $\beta \leq 1$. Then*

$$\begin{aligned}\operatorname{conv}(\mathcal{G}_{\ell,u}) = \{(x,z) \in \mathbb{R}^n_+ \times \mathbb{R} : px_i \leq x_j \leq qx_i, \\ f(x) \geq \ell, \\ \ell \leq z \leq u, \\ z \leq f(x)\}.\end{aligned} \tag{90}$$

Proof. The lower envelope is again (85). If $0 < \ell$, the upper envelope is (69) by Theorem 3.5. If $\ell = 0$, the upper envelope is (72) by Proposition 3.7. In both cases, Lemma 3.8 shows that intersecting the lower and upper envelope hulls gives exactly (90). $\square$

Remark 3.12 (Why the graph hull contains $f(x) \geq \ell$). The condition $f(x) \geq \ell$ in Theorems 3.9 and 3.11 is not inherited from the original graph pointwise. It is the convexified domain condition. Corollary 2.7 states that

$$\operatorname{proj}_x \operatorname{conv}(\mathcal{G}_{\ell,u}) = \operatorname{conv}(T_{\ell,u}) = S_\ell. \tag{91}$$

Thus the projection of the graph hull is a monomial superlevel set, not the bounded annulus $\{\ell \leq f \leq u\} \cap W_{ij}$.

The graph-hull formulas show a separation between domain convexification and vertical convexification. The x-projection is always S_ℓ for $n \geq 3$, independently of u and independently of whether β is above or below one. The vertical upper endpoint, however, depends on both u and β. When $\beta \leq 1$, concavity of the monomial keeps the upper side at $z \leq f(x)$, together with $z \leq u$. When $\beta > 1$, the upper side is the secant-conic function inherited from the known upper envelope. Therefore the complete graph hull is not a trivial cylinder over S_ℓ; only its lower endpoint is flat. This distinction is relevant for relaxations, because a solver that uses the lower theorem alone still needs the upper inequalities to obtain the exact convex hull of the graph.

The formulas are also consistent with the limiting case $\ell = 0$. The lower envelope becomes $z \geq 0$, and the graph hull for $\beta > 1$ reduces to the homogeneous inequality $z^\beta \leq u^{\beta-1} f(x)$ with $0 \leq z \leq u$. No singular term remains because the vertex shift z_0 vanishes in the limit. For $\beta \leq 1$, the concave hypograph description is unchanged. These limiting statements are useful in applications where the lower value bound is a modeling artifact and may be zero.

3.3. Sharpness of the dimension assumption

The preceding proof uses a coordinate outside the pair (i,j). This is not a technical artifact. In dimension two the compensating coordinate does not exist, the level-set identity fails, and the lower envelope is genuinely nontrivial, as shown in.[1] The following example isolates the obstruction.

Example 3.13 (Failure of the level identity in dimension two)**.** Let $n = 2$, $a_1 = a_2 = 1$, $i = 1$, $j = 2$, $p = 1$, and $q = 2$. Then

$$\begin{aligned} &W_{12} = \{(x_1,x_2) \in \mathbb{R}^2_+ : x_1 \leq x_2 \leq 2x_1\}, \\ &f(x) = x_1 x_2. \end{aligned} \tag{92}$$

The level set $L_1 = \{x \in W_{12} : x_1 x_2 = 1\}$ is

$$L_1 = \{(s, rs) : 1 \leq r \leq 2,\ s = r^{-1/2}\}. \tag{93}$$

Consequently,

$$2^{-1/2} \leq x_1 \leq 1, \qquad 1 \leq x_2 \leq 2^{1/2} \quad \text{for all } x \in L_1. \tag{94}$$

and therefore $\operatorname{conv}(L_1)$ is bounded. But

$$S_1 = \{x \in W_{12} : x_1 x_2 \geq 1\} \tag{95}$$

is unbounded; for example $(t,t) \in S_1$ for every $t \geq 1$. Hence

$$\operatorname{conv}(L_1) \neq S_1. \tag{96}$$

The same obstruction holds for arbitrary positive exponents in dimension two. The cone W_{ij} restricts the two coordinates to a bounded ratio. On the level $f(x) = \ell > 0$, that bounded ratio fixes the common scale within bounded limits. Thus the level set cannot generate the unbounded superlevel set by convexification. At level $\xi = 0$, the failure is even simpler: the level set in dimension two is only the origin, while the superlevel set is the whole cone. In dimension $n \geq 3$, the additional coordinate makes it possible to let the constrained pair collapse while the free coordinate increases, producing the two zero-product endpoints in (38).

Proposition 3.14 (Dimension-sharp dichotomy)**.** *Let $0 < p < q$, $a \in \mathbb{R}^2_{++}$, $i = 1$, and $j = 2$. For every $\ell > 0$,*

$$\begin{aligned}\operatorname{conv}\{x \in W_{12} : x_1^{a_1} x_2^{a_2} = \ell\} \subsetneq \\ \{x \in W_{12} : x_1^{a_1} x_2^{a_2} \geq \ell\}.\end{aligned} \tag{97}$$

At level $\xi = 0$ one also has

$$\begin{aligned}\operatorname{conv}\{x \in W_{12} : x_1^{a_1} x_2^{a_2} = 0\} = \{0\} \subsetneq W_{12} \\ = \{x \in W_{12} : x_1^{a_1} x_2^{a_2} \geq 0\}.\end{aligned} \tag{98}$$

By contrast, for every $n \geq 3$ the equality (26) holds for all $\xi \geq 0$.

Proof. For $n = 2$, write $r = x_2/x_1 \in [p, q]$. On the level $x_1^{a_1} x_2^{a_2} = \ell$, we have

$$r^{a_2} x_1^{a_1+a_2} = \ell, \qquad x_1 = \left(\frac{\ell}{r^{a_2}}\right)^{1/(a_1+a_2)}. \tag{99}$$

Since $r \in [p, q]$, both x_1 and $x_2 = rx_1$ are bounded above and below on the level set. Hence its convex hull is bounded. The superlevel set is unbounded because for any fixed $r \in [p, q]$,

$$\begin{aligned} x(t) &= (t, rt), \\ f(x(t)) &= r^{a_2} t^{a_1+a_2} \to \infty \quad \text{as } t \to \infty. \end{aligned} \tag{100}$$

Thus the inclusion is strict. For the zero level, if $x_1^{a_1} x_2^{a_2} = 0$, then $x_1 = 0$ or $x_2 = 0$. If $x_1 = 0$, the cone inequality $x_2 \leq qx_1$ gives $x_2 = 0$; if $x_2 = 0$, the cone inequality $px_1 \leq x_2$ gives $x_1 = 0$. Hence the zero level set is $\{0\}$, while $S_0 = W_{12}$ contains nonzero points, for instance $(1, p)$. This proves (98). The statement for $n \geq 3$ is Theorem 2.5. □

3.4. Numerical experiments and visual checks

The numerical experiments are designed to complement, not replace, the analytical proof. The first experiment follows the proof along a single compensating-coordinate path; the second visualizes the flat lower envelope on a two-dimensional slice; the third contrasts the $n \geq 3$ identity with the failure in dimension two; the fourth stress-tests the constructive certificates over randomly generated points; and the fifth displays the vertical graph-hull fiber for the case $\beta > 1$. The tested regimes are listed in **Table 1**. Cases A and C have $\beta > 1$, Case B has $\beta < 1$, and Case D is a heterogeneous ten-dimensional instance intended to test scaling behavior. The chosen parameters are not tuned to produce favorable residuals. They include both concave and nonconcave monomial regimes, narrow and wide ratio cones, and a ten-dimensional exponent vector with entries ranging from 0.20 to 1.75. This variety is useful because the path profile can become steep near the level roots when β is large, whereas the lower-envelope theorem itself is insensitive to β.

Two kinds of visual information are reported. The surface plots illustrate the geometric statement of the theorem on low-dimensional slices that can be drawn. The residual plots and tables instead inspect the constructive certificate in dimensions where direct visualization is impossible. In all cases the tested statement is the same: the sampled point $x \in S_\ell$ must be expressible as $\lambda y^- + (1 - \lambda) y^+$ with $y^-, y^+ \in L_\ell$. The numerical values in the tables should therefore be read as reproducibility diagnostics for the formula, not as empirical evidence for a conjecture.

Table 1. Parameter regimes used in the numerical experiments

Case	n	β	p	q	ℓ	u
A	3	2.60	0.35	3.00	0.40	10.00
B	3	0.85	0.40	3.30	0.65	1.21
C	5	4.60	0.20	5.00	1.00	20.00
D	10	8.50	0.15	7.50	0.80	30.00

Figure 1 shows the univariate monomial value along the affine path used in the proof for Case A. The profile is zero at both endpoints of the feasible interval, exceeds ℓ at the input point $t = 0$, and crosses the target level twice. The two crossing points are the endpoints y^- and y^+ of the certificate; the original point is recovered by the barycentric coefficient $\lambda = t^+/(t^+ - t^-)$.

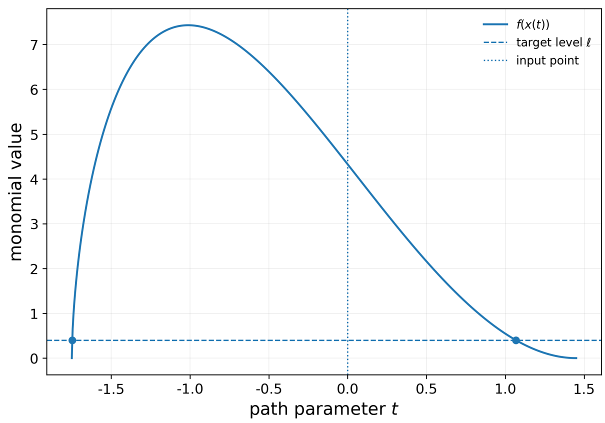

Figure 1. Two-point level certificate along the compensating-coordinate path. The dashed horizontal line is the target level ℓ, the dotted vertical line is the sampled point, and the marked intersections give y^- and y^+.

Figure 2 visualizes a slice of the lower envelope for Case A with fixed ratio $x_j = 1.45x_i$. The curved surface is the original monomial graph on the slice, while the planar surface is $z = \ell$ restricted to the convexified projection $f(x) \geq \ell$. The picture illustrates the main theorem: after convexification, the lower side does not follow the curvature of f; it is the flat lower value bound on the whole superlevel domain.

Figure 3 shows the obstruction in dimension two for $f(x) = x_1 x_2$, $p = 1$, $q = 2$, and $\ell = 1$. The level set inside the cone is bounded, whereas the superlevel set extends indefinitely along every ray $x_2 = rx_1$ with $r \in [p, q]$. This visualization corresponds to Example 3.13 and explains why the compensating coordinate in Theorem 2.5 is not a proof artifact.

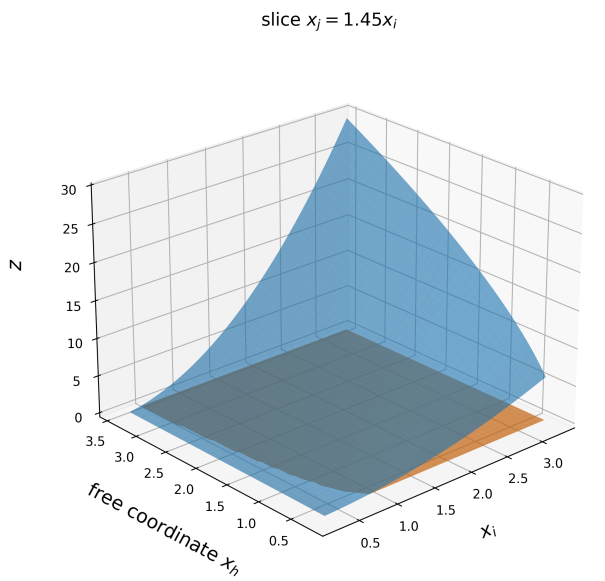

Figure 2. Flat lower envelope on a two-dimensional slice of a three-dimensional instance. The lower surface is the plane $z = \ell$ over the convexified projection $\{x \in W_{ij} : f(x) \geq \ell\}$.

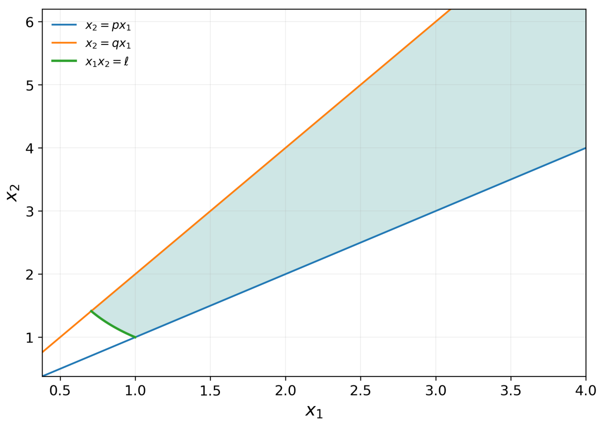

Figure 3. Dimension-two failure of the level-set identity. The shaded region is the truncated view of $\{x \in W_{12} : x_1x_2 \geq 1\}$, while the curve is the bounded level set $x_1x_2 = 1$ inside the cone.

For each case in **Table 1**, 2,000 points were sampled from S_ℓ and decomposed by the logarithmic bisection protocol. **Table 2** reports the median barycentric coefficient, the median value of $f(x)/\ell$, the maximum relative reconstruction residual, the maximum relative level residual, and the median runtime per certificate. The reconstruction error stays at floating-point precision in every regime. The endpoint level residual is also small; the largest value occurs in the high-degree ten-dimensional case and remains below 5×10^{-7} for the tested sample.

The empirical cumulative distribution in **Figure 4** gives the full distribution of reconstruction residuals from the same stress test. The plot confirms that the two-point certificate is numerically stable across low- and higher-dimensional regimes, including heterogeneous exponent vectors.

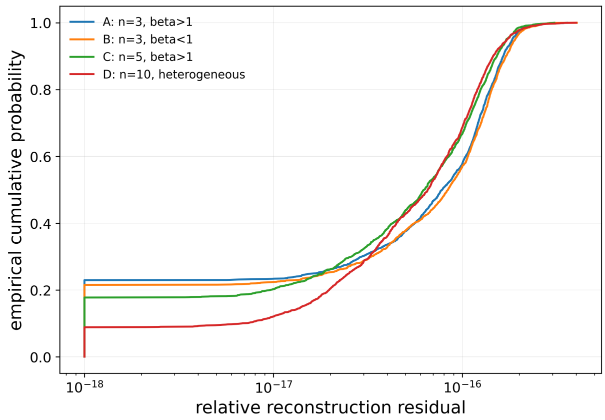

Figure 4. Empirical cumulative distribution of the relative reconstruction residual in the two-point certificate stress test

Finally, **Figure 5** displays the vertical fiber implied by the graph hull in the case $\beta > 1$. The lower endpoint is the constant ℓ, while the upper endpoint follows the Belotti secant-conic expression until the value bound u becomes active. This one-dimensional view is useful because the full graph hull lives in $n+1$ dimensions; the vertical fiber summarizes the admissible range of z after the lower and upper envelopes are intersected.

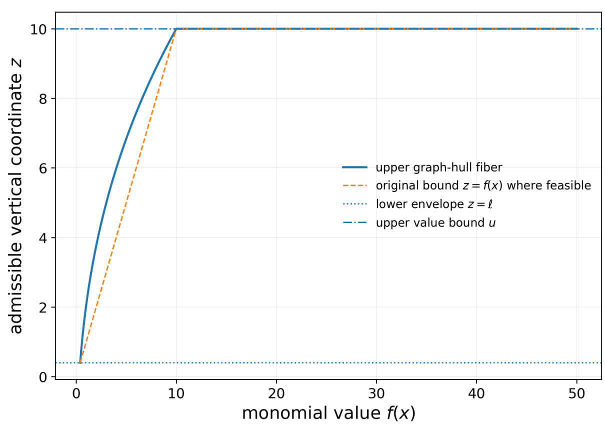

Figure 5. Vertical fiber of the graph hull for a $\beta > 1$ instance as a function of the monomial value $f(x)$. The lower endpoint is $z = \ell$, and the upper endpoint is the minimum of u and the secant-conic upper envelope.

Table 2. Stress-test results for the constructive two-point certificate

Case	Median λ	Median f/ℓ	Max rec. res.	Max level res.	Median ms
A	0.362	5.788	3.59×10^{-16}	3.00×10^{-12}	0.783
B	0.470	2.052	4.04×10^{-16}	6.49×10^{-14}	0.722
C	0.408	4.419	3.07×10^{-16}	1.62×10^{-13}	0.749
D	0.454	18.286	4.01×10^{-16}	4.63×10^{-7}	0.884

4. Discussion

4.1. Constructive decomposition and separation

The proof of Theorem 2.5 is constructive. This section records the explicit decomposition because it is useful for checking membership, certifying lower-envelope points, and generating primal convex combinations.

Let $x \in S_\ell$. If $f(x) = \ell$, then the trivial certificate is

$$x = 1 \cdot x, \qquad x \in L_\ell. \tag{101}$$

Assume $f(x) > \ell$. Choose any $h \in N \setminus \{i, j\}$ and set $r = x_j/x_i$. Define $x(t)$ and $\phi(t)$ as in (31)–(37). We need two roots of

$$\phi(t) = \ell \tag{102}$$

in the intervals $[-x_h, 0]$ and $[0, x_i]$. Writing

$$\begin{aligned} C &:= r^{a_j} \prod_{k \in N\setminus\{i,j,h\}} x_k^{a_k} > 0, \\ A &:= a_i + a_j, \qquad B := a_h. \end{aligned} \tag{103}$$

the equation is

$$C(x_i - t)^A (x_h + t)^B = \ell. \tag{104}$$

There is no need for a closed-form solution. If $\ell = 0$, the endpoint choices

$$t^- = -x_h, \qquad t^+ = x_i \tag{105}$$

solve (102). If $\ell > 0$, the function is continuous, equals 0 at each endpoint, and is above ℓ at $t = 0$; hence the intermediate value theorem gives exact roots $t^- \in (-x_h, 0)$ and $t^+ \in (0, x_i)$. In numerical implementations, bisection can approximate these roots to any prescribed tolerance. When logarithmic values are used, the bisection is performed only on the open intervals $(-x_h, 0)$ and $(0, x_i)$, with the endpoint values treated as one-sided limits, so that $\log x_k(t)$ is never evaluated at a zero coordinate. Once exact roots t^- and t^+ are fixed, the decomposition is

$$y^- := x(t^-), \qquad y^+ := x(t^+), \tag{106}$$

$$\lambda := \frac{t^+}{t^+ - t^-}, \tag{107}$$

$$x = \lambda y^- + (1-\lambda) y^+, \qquad f(y^-) = f(y^+) = \ell. \tag{108}$$

Given such a certificate for $x \in S_\ell$, the lifted point (x, z) belongs to the lower epigraph hull if and only if $z \geq \ell$. Equivalently,

$$(x, z) \in \operatorname{conv}(\operatorname{epi}(f, T_{\ell,u})) \iff x \in S_\ell \text{ and } z \geq \ell. \tag{109}$$

The resulting certificate-generation procedure is summarized in **Algorithm 1**.

Algorithm 1. Two-point decomposition scheme for the lower envelope

Require: $x \in \mathbb{R}^n$, indices $i \neq j$, constants $0 < p < q$, exponent vector $a \in \mathbb{R}^n_{++}$, lower level $\ell \geq 0$, and, for numerical use, an optional tolerance $\varepsilon > 0$.
Ensure: Either an exact certificate $x = \lambda y^- + (1-\lambda)y^+$ with $y^\pm \in L_\ell$ if the root equations are solved exactly, an ε-approximate certificate in numerical mode, or a declaration that $x \notin S_\ell$.

```
if x_k < 0 for some k ∈ N then
    declare x ∉ S_ℓ and stop.
end if
if p x_i > x_j or x_j > q x_i or f(x) < ℓ then
    declare x ∉ S_ℓ and stop.
end if
if f(x) = ℓ then
    set y⁻ = y⁺ = x and λ = 1; stop.
end if
choose h ∈ N \ {i, j} and set r = x_j/x_i.
define x(t) by (31)–(34).
if ℓ = 0 then
    set t⁻ = −x_h and t⁺ = x_i.
else
    find t⁻ ∈ (−x_h, 0) and t⁺ ∈ (0, x_i) satisfying f(x(t⁻)) = f(x(t⁺)) = ℓ by exact root solving, or approximate them by bisection to tolerance ε.
end if
set y⁻ = x(t⁻), y⁺ = x(t⁺), and λ = t⁺/(t⁺ − t⁻).
return the exact certificate x = λy⁻ + (1−λ)y⁺ if exact roots were used; otherwise return the corresponding approximate certificate.
```

The separation problem for the lower envelope is correspondingly simple. The closed convex set in Theorem 3.1 is

$$\begin{aligned} K^- := \{(x, z) : x \in \mathbb{R}^n_+,\ p x_i \leq x_j \leq q x_i, \\ f(x) \geq \ell,\ z \geq \ell\}. \end{aligned} \tag{110}$$

Membership requires checking the two linear inequalities, nonnegativity, the scalar lower bound on z, and the monomial superlevel inequality. For $\ell > 0$, the latter can be written as

$$\sum_{k=1}^{n} a_k \log x_k \geq \log \ell, \qquad x \in \mathbb{R}^n_{++}. \tag{111}$$

A violated superlevel inequality at a strictly positive point admits a separating hyperplane generated by the convex function

$$\psi(x) := \log \ell - \sum_{k=1}^{n} a_k \log x_k, \qquad x \in \mathbb{R}^n_{++}. \tag{112}$$

Indeed, if $\bar{x} \in \mathbb{R}^n_{++}$ and $f(\bar{x}) < \ell$, then $\psi(\bar{x}) > 0$ and convexity of ψ gives the separating inequality

$$\psi(\bar{x}) + \nabla\psi(\bar{x})^\top (x - \bar{x}) \leq 0, \tag{113}$$

valid for S_ℓ and violated by $\bar{x}$. Since

$$\nabla\psi(\bar{x}) = -\left(\frac{a_1}{\bar{x}_1}, \dots, \frac{a_n}{\bar{x}_n}\right), \tag{114}$$

(113) is explicitly

$$\log \ell - \sum_{k=1}^{n} a_k \log \bar{x}_k - \sum_{k=1}^{n} \frac{a_k}{\bar{x}_k}(x_k - \bar{x}_k) \leq 0. \tag{115}$$

If $\bar{x} \in \mathbb{R}^n_+ \setminus \mathbb{R}^n_{++}$ and $\ell > 0$, then $f(\bar{x}) = 0 < \ell$ and $\bar{x} \notin S_\ell$. Since S_ℓ is closed and convex, a separating hyperplane exists by the strong separation theorem. Equivalently, if $\hat{x}$ is the Euclidean projection of $\bar{x}$ onto S_ℓ, then

$$(\hat{x} - \bar{x})^\top (x - \hat{x}) \geq 0 \tag{116}$$

is valid for every $x \in S_\ell$ and is violated by $x = \bar{x}$. The explicit log-gradient separator (115) is intended only for the strictly positive case $\bar{x} \in \mathbb{R}^n_{++}$.

Proposition 4.1 (Lower-envelope separation). *For $\ell > 0$, a point $(\bar{x}, \bar{z}) \in \mathbb{R}^n \times \mathbb{R}$ violates* $\operatorname{conv}(\operatorname{epi}(f, T_{\ell,u}))$ *if and only if at least one of the following conditions holds:*

$$\bar{x}_k < 0 \quad \textit{for some } k, \tag{117}$$

$$p\bar{x}_i > \bar{x}_j, \quad \textit{or} \quad \bar{x}_j > q\bar{x}_i, \tag{118}$$

$$\bar{x} \in \mathbb{R}^n_+ \textit{ and } f(\bar{x}) < \ell, \tag{119}$$

$$\bar{z} < \ell. \tag{120}$$

Each violation yields a separating hyperplane: coordinate nonnegativity gives the hyperplane for (117)*; one of the two cone inequalities gives the hyperplane for* (118)*; when* (119) *holds with $\bar{x} \in \mathbb{R}^n_{++}$, the explicit log separator* (115) *applies; when* (119) *holds with a zero coordinate, the projection separator* (116) *(or any strong-separation hyperplane) applies; and the bound $z \geq \ell$ gives the hyperplane for* (120)*.*

Proof. The equivalence follows directly from the closed-form description (51), with $f(\bar{x})$ evaluated only on $\mathbb{R}^n_+$. The listed inequalities are valid separating inequalities for the corresponding violated closed convex constraints defining K^-. □

4.2. Additional consequences

We record two further consequences that clarify how the lower envelope interacts with other relaxations.

Proposition 4.2 (Persistence under additional level-preserving restrictions). *Let $Y \subseteq W_{ij}$ satisfy*

$$L_\ell \subseteq Y \subseteq S_\ell. \tag{121}$$

Then

$$\operatorname{conv}(Y) = S_\ell, \tag{122}$$

and

$$\operatorname{conv}(\operatorname{epi}(f, Y)) = S_\ell \times [\ell, \infty). \tag{123}$$

In particular, every restriction Y that contains all level-ℓ points and is contained in S_ℓ has the same lower envelope as $T_{\ell,u}$.

Proof. Since $L_\ell \subseteq Y \subseteq S_\ell$ and Theorem 2.5 gives $\operatorname{conv}(L_\ell) = S_\ell$, we have

$$S_\ell = \operatorname{conv}(L_\ell) \subseteq \operatorname{conv}(Y) \subseteq S_\ell. \tag{124}$$

Hence $\operatorname{conv}(Y) = S_\ell$. The inclusion

$$\operatorname{conv}(\operatorname{epi}(f, Y)) \subseteq S_\ell \times [\ell, \infty) \tag{125}$$

follows from $Y \subseteq S_\ell$ and $f \geq \ell$ on Y. For the reverse inclusion, take $(x, z) \in S_\ell \times [\ell, \infty)$. Because $\operatorname{conv}(L_\ell) = S_\ell$, use the same level-$\ell$ decomposition as in Theorem 3.1. Since $L_\ell \subseteq Y$, the two level points are in Y, and the vertical coordinate $z \geq \ell$ makes both lifted points epigraph points. This proves (123). □

Proposition 4.3 (Independence from the chosen free coordinate). *Let $x \in S_\ell$ with $f(x) > \ell$. For every $h \in N \setminus \{i, j\}$, the construction in Theorem 2.5 yields a valid two-point decomposition of x into level-ℓ points. Hence the lower envelope is invariant under the choice of compensating coordinate.*

Proof. The proof of Theorem 2.5 uses no property of h other than the facts that $h \notin \{i, j\}$ and $x_h > 0$. Since $f(x) > \ell \geq 0$ implies $x \in \mathbb{R}^n_{++}$, every such h is admissible. The resulting line segment remains in W_{ij} because it preserves the relation $x_j(t) = r x_i(t)$ with $r \in [p, q]$, with the quotient interpreted only when $x_i(t) > 0$, and its two endpoints have zero monomial value. Thus the intermediate value argument works for each choice of h. □

4.3. Limitations and implications

The result is exact but intentionally specialized. It assumes positive exponents, nonnegative variables, and a single two-variable cone. Negative exponents require a different domain because the monomial is not finite on the boundary of $\mathbb{R}^n_+$. Multiple simultaneous ratio cones can also change the geometry: if every coordinate is tied to the constrained pair, the compensating motion used in Theorem 2.5 may be blocked. Similarly, additional side constraints that remove part of the level set L_ℓ can destroy the identity $\operatorname{conv}(L_\ell) = S_\ell$. Proposition 4.2 gives a precise positive statement: the flat lower envelope persists for any restriction that still contains all level-ℓ points and remains inside S_ℓ.

For global optimization algorithms, the implication is mainly structural. In dimensions at least three, convex strengthening of the lower side of the bounded monomial graph over a two-variable cone is impossible without adding information beyond $T_{\ell,u}$. Algorithmic effort should therefore be directed toward the upper envelope, separation of the convexified projection, and branching rules that reduce the upper-fiber width. The constructive certificate provides an interpretable primal proof of membership in the lower epigraph hull, while the log-gradient separator gives a direct cut when a trial point violates the convexified projection. These components can be embedded in conic, nonlinear, or extended-formulation relaxations without changing the lower-envelope formula.

The flat envelope also clarifies how future computational work should benchmark relaxations that use ratio cones. If a relaxation is weak on instances with $n \geq 3$, the weakness cannot be attributed to a missing convex lower monomial cut of the same variable set, because the strongest possible convex lower-side cut is already known. Any improvement must come from combining several terms, adding side constraints, tightening the upper envelope, or choosing a partition that reduces the feasible vertical interval. Conversely, when a model contains a two-dimensional monomial term without a compensating coordinate, the lower envelope remains genuinely curved and the present theorem does not replace the dimension-two formula. This separation of regimes should help avoid unnecessary cut generation in higher-dimensional terms while preserving specialized treatment for two-dimensional terms.

5. Conclusion

The lower envelope open problem left in[1] for bounded monomials on two-variable cones in dimension $n > 2$ has a simple but structurally strong answer: the lower convex envelope is flat. The exact epigraph hull is

$$\begin{aligned}\operatorname{conv}(\operatorname{epi}(f, X_{\ell,u} \cap W_{ij})) \\ = \{(x,z) : x \in W_{ij}, \\ f(x) \geq \ell,\ z \geq \ell\}.\end{aligned} \tag{126}$$

The proof reduces the problem to the level-set identity

$$\operatorname{conv}\{x \in W_{ij} : f(x) = \xi\} = \{x \in W_{ij} : f(x) \geq \xi\}, \quad \xi \geq 0. \tag{127}$$

which is established by a two-point construction using one coordinate outside the constrained pair. This explains both why the $n = 2$ case is exceptional and why the lower envelope for every $n \geq 3$ is independent of the upper monomial bound u. Together with the known upper envelope, the result gives the complete convex hull of the bounded graph over W_{ij} in all dimensions at least three.

Notations

Symbol	Meaning
N	Index set $\{1, \ldots, n\}$.
i, j	Distinct indices defining the two-variable cone.
h	Compensating coordinate chosen from $N \setminus \{i, j\}$.
a; β	Positive exponent vector; total homogeneity degree $\sum_k a_k$.
$f(x)$	Monomial $\prod_k x_k^{a_k}$ with the boundary convention $0^\alpha = 0$.
W_{ij}	Cone $\{x \in \mathbb{R}^n_+ : px_i \leq x_j \leq qx_i\}$.
$X_{\ell,u}$	Bounded monomial set $\{x \in \mathbb{R}^n_+ : \ell \leq f(x) \leq u\}$.
$T_{\ell,u}$	Restricted feasible set $X_{\ell,u} \cap W_{ij}$.
L_ξ; S_ξ	Monomial level set and superlevel set inside W_{ij}.
$\mathcal{E}^-$; $\mathcal{E}^+$	Convexified restricted epigraph and hypograph.
$\mathcal{G}_{\ell,u}$	Bounded graph of f over $T_{\ell,u}$.
r	Fixed ratio x_j/x_i used along the path construction.
t^-, t^+	Two roots producing the level-set certificate.

Acknowledgments

None.

Funding

None.

Conflict of interest

The authors declare no conflicts of interest.

Author contributions

Conceptualization: All authors
Methodology: All authors
Formal analysis: All authors
Validation: All authors
Visualization: All authors
Writing—original draft: All authors
Writing—review & editing: All authors

Availability of data

All data reported in the numerical experiments are synthetic and can be regenerated by the Python script supplied with the manuscript. The generated summary file is included as `data/certificate_stress_summary.csv`. The supplied Python script is included in the source package for reproducibility. It generates the figures and numerical summaries reported in Section 3.4.

AI tools statement

OpenAI GPT-5.5 Pro was used, under the authors' supervision, for (i) language editing and structural formatting, (ii) assistance in preparing reproducible numerical-illustration code, and (iii) exploratory counterexample search as well as the generation and comparison of candidate proof strategies/proof sketches. All AI-suggested counterexamples, proof outlines, symbolic steps, and numerical results were independently re-derived, verified, or discarded by the authors; every figure and computation appearing in the final manuscript was produced and checked by the authors. The authors reviewed and verified all mathematical arguments, computations, figures, and conclusions, and remain fully responsible for the content of the manuscript. No artificial intelligence tool is listed as an author or co-author.

References

1. Belotti P. Convex envelopes of bounded monomials on two-variable cones. *Math Program.* 2025;211(1–2):93–123. https://doi.org/10.1007/s10107-025-02212-5
2. McCormick GP. Computability of global solutions to factorable nonconvex programs: Part I–Convex underestimating problems. *Math Program.* 1976;10(1):147–175. https://doi.org/10.1007/BF01580665
3. Al-Khayyal FA, Falk JE. Jointly constrained biconvex programming. *Math Oper Res.* 1983;8(2):273–286. https://doi.org/10.1287/moor.8.2.273
4. Rikun AD. A convex envelope formula for multilinear functions. *J Glob Optim.* 1997;10(4):425–437. https://doi.org/10.1023/A:1008217604285
5. Meyer CA, Floudas CA. Trilinear monomials with mixed sign domains: Facets of the convex and concave envelopes. *J Glob Optim.* 2004;29(2):125–155. https://doi.org/10.1023/B:JOGO.0000042112.72379.e6
6. Anstreicher KM, Burer S, Park K. Convex hull representations for bounded products of variables. *J Glob Optim.* 2021;80:757–778. https://doi.org/10.1007/s10898-021-01046-7
7. Nguyen TT, Richard J-PP, Tawarmalani M. Deriving convex hulls through lifting and projection. *Math Program.* 2018;169(2):377–415. https://doi.org/10.1007/s10107-017-1138-3
8. Tawarmalani M, Sahinidis NV. *Convexification and Global Optimization in Continuous and Mixed-Integer Nonlinear Programming.* Kluwer Academic Publishers; 2002. https://doi.org/10.1007/978-1-4757-3532-1
9. He T, Tawarmalani M. A new framework to relax composite functions in nonlinear programs. *Math Program.* 2021;190:427–466. https://doi.org/10.1007/s10107-020-01541-x
10. Kim J, Richard J-PP, Tawarmalani M. Piecewise polyhedral relaxations of multilinear optimization. *SIAM J Optim.* 2024;34(4):3167–3193. https://doi.org/10.1137/22M1507486
11. Horst R, Tuy H. *Global Optimization: Deterministic Approachesn*, 3rd rev. and enl. ed. Springer; 1996. https://doi.org/10.1007/978-3-662-03199-5
12. Sherali HD, Adams WP. *A Reformulation-Linearization Technique for Solving Discrete and Continuous Nonconvex Problems.* Kluwer Academic Publishers; 1999. https://doi.org/10.1007/978-1-4757-4388-3
13. Belotti P, Lee J, Liberti L, Margot F, Wächter A. Branching and bounds tightening techniques for non-convex MINLP. *Optim Methods Softw.* 2009;24(4–5):597–634. https://doi.org/10.1080/10556780903087124
14. Smith EMB, Pantelides CC. A symbolic reformulation/spatial branch-and-bound algorithm for the global optimisation of nonconvex MINLPs. *Comput Chem Eng.* 1999;23(4–5):457–478. https://doi.org/10.1016/S0098-1354(98)00286-5
15. Sahinidis NV. BARON: A general purpose global optimization software package. *J Glob Optim.*

1996;8(2):201–205.
https://doi.org/10.1007/BF00138693

16. Misener R, Floudas CA. ANTIGONE: Algorithms for continuous/integer global optimization of nonlinear equations. *J Glob Optim.* 2014;59(2–3):503–526.
https://doi.org/10.1007/s10898-014-0166-2

17. Bestuzheva K, Besançon M, Chen W-K, et al. The SCIP Optimization Suite 8.0. *arXiv.* Published 2021. https://arxiv.org/abs/2112.08872

18. Irkıl N, Pişkin E, Agarwal P. Global existence and decay of solutions for a system of viscoelastic wave equations of Kirchhoff type with logarithmic nonlinearity. *Math Methods Appl Sci.* 2022;45(5):2921–2948.
https://doi.org/10.1002/mma.7964

19. Rajchakit G, Sriraman R, Boonsatit N, Hammachukiattikul P, Lim CP, Agarwal P. Global exponential stability of Clifford-valued neural networks with time-varying delays and impulsive effects. *Adv Differ Equ.* 2021;2021:208.
https://doi.org/10.1186/s13662-021-03367-z

20. Zhang Y, Agarwal P, Bhatnagar V, Balochian S, Yan J. Swarm intelligence and its applications. *Sci World J.* 2013;2013:528069.
https://doi.org/10.1155/2013/528069

21. Zhang Y, Agarwal P, Bhatnagar V, Balochian S, Zhang X. Swarm Intelligence and Its Applications 2014. *Sci World J.* 2014;2014:204294.
https://doi.org/10.1155/2014/204294

22. Saber S. Solution to $\bar{\partial}$-problem with support conditions in weakly q-convex domains. *Commun Korean Math Soc.* 2018;33(2):409–421.
https://doi.org/10.4134/CKMS.c170022

23. Saber S. Compactness of commutators of Toeplitz operators on q-pseudoconvex domains. *Electron J Differ Equ.* 2018;2018(111):1–17. Accessed June 10, 2026. https://hdl.handle.net/10877/15302

24. Saber S. Compactness of the complex Green operator in a Stein manifold. *UPB Sci Bull Ser A.* 2019;81(2):185–200. Accessed June 10, 2026. https://www.scientificbulletin.upb.ro/static/pdfs/rez625_100458.pdf

25. Boyd S, Kim S-J, Vandenberghe L, Hassibi A. A tutorial on geometric programming. *Optim Eng.* 2007;8(1):67–127.
https://doi.org/10.1007/s11081-007-9001-7

26. Ecker JG. Geometric programming: Methods, computations and applications. *SIAM Rev.* 1980;22(3):338–362.
https://doi.org/10.1137/1022058

27. Duffin RJ, Peterson EL, Zener C. *Geometric Programming: Theory and Application.* Wiley; 1967.

28. Boyd SP, Kim S-J, Patil DD, Horowitz MA. Digital circuit optimization via geometric programming. *Oper Res.* 2005;53(6):899–932.
https://doi.org/10.1287/opre.1050.0254

29. Hershenson MDM, Boyd SP, Lee TH. Optimal design of a CMOS op-amp via geometric programming. *IEEE Trans Comput-Aided Des Integr Circuits Syst.* 2001;20(1):1–21.
https://doi.org/10.1109/43.905671

30. Hoburg W, Abbeel P. Geometric programming for aircraft design optimization. *AIAA J.* 2014;52(11):2414–2426.
https://doi.org/10.2514/1.J052732

31. Ogura M, Kishida M, Lam J. Geometric programming for optimal positive linear systems. *IEEE Trans Autom Control.* 2020;65(11):4648–4663.
https://doi.org/10.1109/TAC.2019.2960697

32. Lu H-C, Li H-L, Gounaris CE, Floudas CA. Convex relaxation for solving posynomial programs. *J Glob Optim.* 2010;46(1):147–154.
https://doi.org/10.1007/s10898-009-9414-2

33. Tsai J-F, Lin M-H. An efficient global approach for posynomial geometric programming problems. *INFORMS J Comput.* 2011;23(3):483–492.
https://doi.org/10.1287/ijoc.1100.0403

34. Neumaier A. *Interval Methods for Systems of Equations.* Cambridge University Press; 1990.
https:///doi.org/10.1017/CBO9780511526473

35. Lee J, Skipper D, Speakman E. Algorithmic and modeling insights via volumetric comparison of polyhedral relaxations. *Math Program.* 2018;170(1):121–140.
https://doi.org/10.1007/s10107-018-1272-6

36. Speakman E, Lee J. Quantifying double McCormick. *Math Oper Res.* 2017;42(4):1230–1253.
https://doi.org/10.1287/moor.2017.0846

37. Speakman E, Lee J. On branching-point selection for trilinear monomials in spatial branch-and-bound: The hull relaxation. *J Glob Optim.* 2018;72(2):129–153.
https://doi.org/10.1007/s10898-018-0620-7

38. Lee J, Skipper D, Speakman E. Gaining or losing perspective. *J Glob Optim.* 2022;82:835–862.
https://doi.org/10.1007/s10898-021-01055-6

39. Rockafellar RT. *Convex Analysis.* Princeton University Press; 1970. URL: https://www.jstor.org/stable/j.ctt14bs1ff

40. Hiriart-Urruty J-B, Lemaréchal C. *Convex Analysis and Minimization Algorithms I: Fundamentals.* Springer; 1993.
https://doi.org/10.1007/978-3-662-02796-7

41. Boyd S, Vandenberghe L. *Convex Optimization.* Cambridge University Press; 2004.
https://doi.org/10.1017/CBO9780511804441

42. Ben-Tal A, Nemirovski A. *Lectures on Modern Convex Optimization*. SIAM; 2001. https://doi.org/10.1137/1.9780898718829

43. Bénichou M, Gauthier JM, Girodet P, Hentges G, Ribière G, Vincent O. Experiments in mixed-integer linear programming. *Math Program.* 1971;1(1):76–94. https://doi.org/10.1007/BF01584074

44. Belotti P, Góez JC, Pólik I, Ralphs TK, Terlaky T. A complete characterization of disjunctive conic cuts for mixed integer second order cone optimization. *Discret Optim.* 2017;24:3–31. https://doi.org/10.1016/j.disopt.2016.10.001

45. Speakman E, Yu H, Lee J. Experimental validation of volume-based comparison for double-McCormick relaxations. In: Salvagnin D, Lombardi M, editors. *Integration of AI and OR Techniques in Constraint Programming.* CPAIOR 2017. Lecture Notes in Computer Science, vol 10335. Springer; 2017:229–243. https://doi.org/10.1007/978-3-319-59776-8_19

Yutong Zhang *is an undergraduate student at the School of Mathematics, Sichuan University, Chengdu, China.*

Yaoran Yang *is an undergraduate student at the School of Mathematics, Sichuan University, Chengdu, China.*

An International Journal of Optimization and Control: Theories & Applications (https://accscience.com/journal/ijocta)